Cooperative Observations by Photogrammetric Methods with the TOM Satellite Formation

Jonas Jensen [(1)], Johannes Dauner[(1)], Alexander Kleinschrodt[(1)], Ilham Mammadov[(2)], Prachit Kamble[(2)], Lisa Elsner[(1)], Klaus Schilling[(1)]

[(1)] Zentrum für Telematik (ZfT), {firstname.lastname}@telematik-zentrum.de
[(2)] S [4] - Smart Small Satellite Systems GmbH, {firstname.lastname}@s4-space.com

ABSTRACT

Characterization of 3-dimensional phenomena in the Earth's atmosphere and on its surface can be addressed by combination of camera images simultaneously taken from different perspectives. The TOM formation, composed of 3 small satellites, uses sensor data fusion by photogrammetric methods to generate 3D-images for assessment of spatial distribution of objects. Typical application scenarios include detection and analyses of ash clouds from volcano eruptions, of contrails generated by aircrafts, or of ice floes calving from glaciers into the sea. The satellite hardware has been completed and the 3 satellites wait in the cleanroom of Center for Telematics for an expected launch at end of 2024. TOM's payload is a redundant camera system. The satellites will be placed in a triple pendulum configuration for efficient fuel use in formation maintenance. The TOM mission will analyse for different application scenarios optimal selection of crucial parameters to acquire by the formation appropriate inputs for subsequent 3-dimensional image processing. Challenges for satellite system design are related to implementation of formation capabilities at nanosatellite level, in particular for accurate attitude control. It includes a propulsion system for orbit control and maintenance, inter-satellite links for formation coordination, and miniature reaction wheels for pointing. Due to uncertainties in target area position, autonomous and situation aware adaptive control schemes are implemented. Inputs to the control system are provided by GNSS, gyros, magnetometers, and Sun sensors. Payload experiments on improved precision pointing relate to autonomous landmark detection in payload data for fine pointing, based on visual servoing principles. This innovative, cooperative attitude and orbit control system had been tested and characterized first in software simulations, and subsequently in complex Hardware-in-the-Loop (HiL)-tests for integrated satellites at formation level by a combination of two precision turntables. The hardware of the 3 satellites for the TOM formation is completed and is ready for launch.

1 INTRODUCTION

Miniaturization approaches are revolutionizing small satellite capabilities leading to professional cost-efficient satellites with just a few kilograms of mass [17], [26]. This trend opens up exciting possibilities for multi-satellite missions [23], in particular for distributed Earth observation activities [8, 17, 21]. Innovative small satellite techniques enable multi-satellite networks, either in form of ***constellations***, where each satellite is individually controlled from the ground, or in form of more advanced self-organizing ***formations*** [1, 3, 8, 16, 23]. By coordinating payload pointing via inter-satellite links, these cooperative formations enable simultaneous tracking of Earth surface targets from various satellite perspectives. The Telematics Earth Observation Mission (TOM) exemplifies such a formation, allowing the generation of 3D Earth surface images using photogrammetric methods (see Figure 1). This paper presents in this context details of the TOM mission and its satellite design. It addresses the challenging formation control aspects, as well as the payload experiments related to vision-based attitude control.

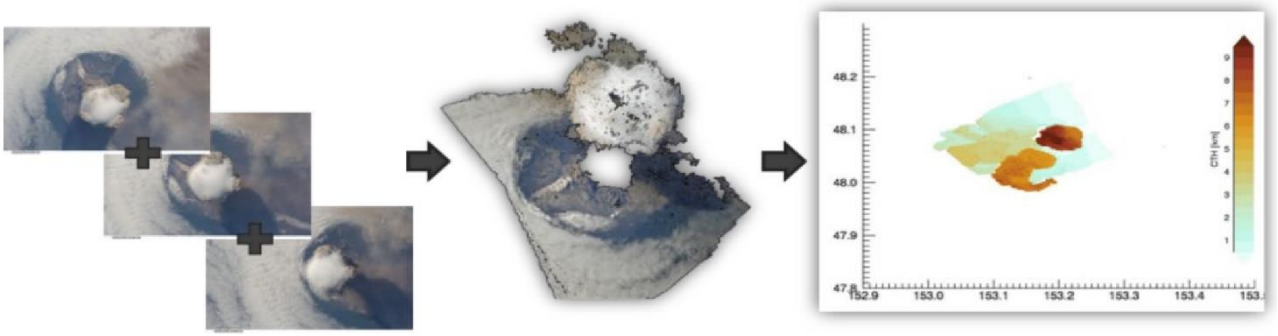

Figure 1: Multiple pictures taken of a volcano eruption from ISS. During ISS's fly-over different viewing angles result, which were taken for testing the TOM image processing software for generating a 3D-image and retrieving information as Cloud Top Height (CTH) .

2 MISSION OBJECTIVES

TOM aims to revolutionize Earth observation by leveraging photogrammetric techniques to acquire high-resolution 3D images of our planet. Achieving this objective involves deploying a nanosatellite formation that synchronously observes target areas on Earth's surface from diverse viewing angles. The central focus of TOM is to monitor and capture real-time images of ash clouds resulting from volcanic eruptions. These ash clouds significantly impact neighboring regions and disrupt aerial transportation. Preparatory image processing tests have already been conducted using camera data from the International Space Station [25] (cf. Figure 1). Modeling these ash clouds in 3D requires addressing the challenges posed by varying altitudes due to wind dynamics. TOM seeks to achieve a sufficient vertical resolution to accurately represent these dynamic structures. Traditional single-satellite overflights struggle to capture rapidly evolving surface features and suffer from parallax effects. TOM addresses this limitation by employing formation flying technologies. By coordinating multiple satellites, the mission enables simultaneous observations of target areas from distinct viewing angles. This cooperative approach enhances data collection efficiency and provides a more comprehensive view of Earth's surface. A critical trade-off exists between data quality and mission cost. To optimize this balance, TOM employs a 3-nano-satellite formation. By adding a third perspective, TOM minimizes occluded areas and maximizes coverage. Height resolution depends on parameters such as GSD, orbit altitude, and baseline distance between satellites.
TOM represents Bavaria's contribution to the Telematics International Mission (TIM) project. Initiated by the Regional Leaders Summit (RLS), this collaborative effort involves space research institutes from partner regions worldwide, collectively forming a Ground Station Network (GSNW) spanning five continents [23].

2.1 CHALLENGES

Challenges concern accommodation of miniaturized satellite components in the limited volume of a 3U- Cubesat to provide all necessary functionalities. These components include attitude control based on micro-reaction wheels for precise pointing during target tracking. The propulsion system is providing the orbit control capability for formation flight. An omni-directional communication unit for Telemetry and Telecommand (TMTC) operates in the UHF band. A high data throughput transmitter in S-band is used for image data transfer. The payload is a redundant camera system based on COTS components. Taking advantage of the cameras additional technology experiments address vision-based control approaches.

3 SATELLITE DESIGN

ZfT has developed a 3U+ satellite platform design that adheres to the UNISEC Europe standard for electrical interfaces[1] (see [2]). This streamlined design facilitates rapid integration and testing of satellite components, while ensuring compatibility across various missions. All subsystems of the satellite are modularly attached to a baseplate (see Figure 2). Within the bottom 10 cm cube, essential avionics components reside, including the On-Board Computer (OBC), Attitude and Orbit Control System (AOCS), Electronic Power System (EPS), and Communication subsystem (COM) while the top unit accommodates the propulsion system. To mitigate single points of failure, redundancy is implemented across all components except the propulsion system, and software-based Fault Detection Identification and Recovery (FDIR) techniques are used. For instance, the OBC features two microcontrollers operating in hot redundancy, monitored externally by a watchdog. The AOCS also adheres to redundancy principles, spanning from microcontroller redundancy to sensor and actuator redundancy.
Furthermore, the distributed EPS architecture effectively isolates power-related failures and tolerates multiple single failures, ensuring mission continuity even in the presence of defects.

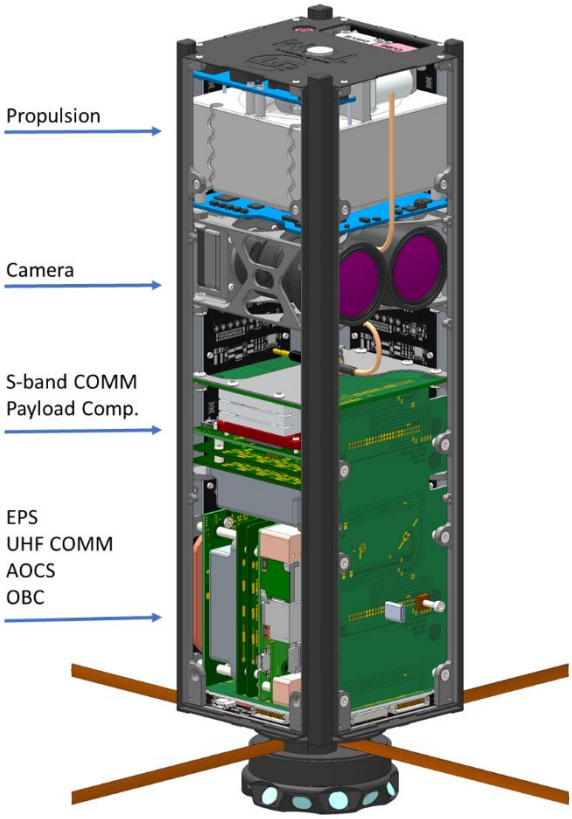

Figure 2: TOM satellite in flight configuration

3.1 PAYLOAD

The redundant camera system for TOM was developed by ZfT. It utilizes a Component of the shelf (COTS) industrial machine vision sensor module paired with a ruggedized lens (see Figure 3). Component selection prioritized maximizing resolution within the TOM satellite's payload volume while meeting mission requirements. The sensor module is equipped with a global shutter image sensor and a data interface supporting MIPI CSI-2. The selection of the optical lens has been optimised for the longest focal length, with the ability to accommodate two lens units side by side in a volume of 95 mm x 95 mm x 45 mm. The payload camera is designed to achieve a GSD of 20 meters and a dispersion of 50 kilometres at an orbital altitude of 600 kilometres. Previous analysis indicates that a 20-meter GSD and a 100-kilometer formation baseline distance suffice for achieving a vertical resolution of 200 meters after photogrammetry (see figure 4). Both the camera system and the payload computer subsystem (PC) underwent radiation testing to ensure durability in the challenging space environment of Low Earth Orbit (LEO). Remarkably, both devices withstood a total ionizing dose of 33 krad.

[1] http://unisec-europe.eu/standards/bus/

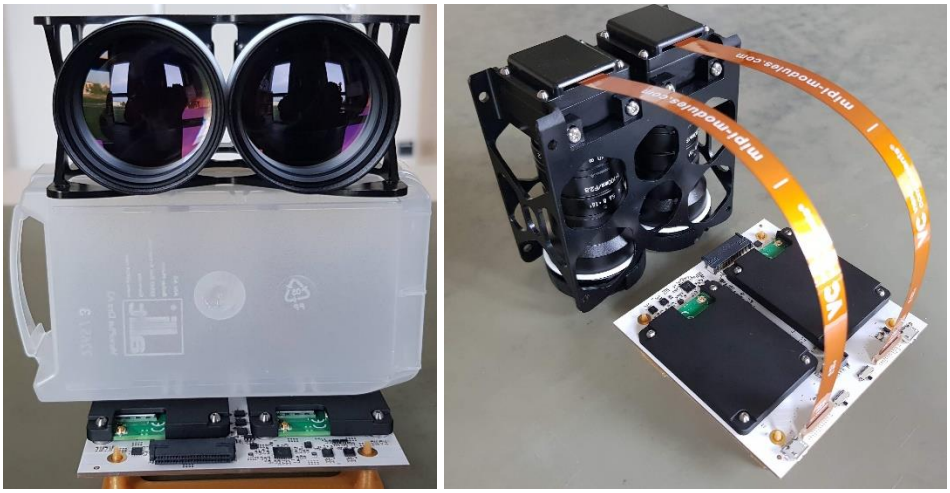

Figure 3 Redundant Camera Unit (left) and Cameras including Payload (right)

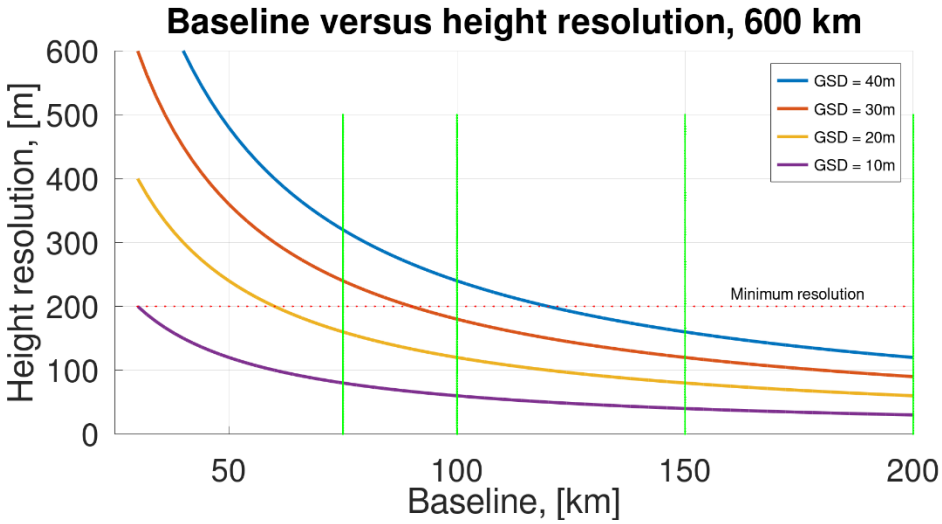

Figure 4 Height resolution dependency on the formation baseline distance

3.2 ADCS

The TOM satellite's attitude control relies on six miniature reaction wheels, with two aligned along each orthogonal axis (see figure 5). This configuration enhances agility while providing redundancy. We strategically positioned the reaction wheels, leaving extra space for piggyback boards that interface with external components of the AOCS, e.g. the propulsion system. Additionally, TOM accommodates a Linux-based computing board to handle mission-specific tasks, such as formation flying. This demanding computation typically exceeds the capabilities of onboard microcontrollers.
A distributed sensor suit together with actuators are placed on the panels of the satellite. This includes five magnetorquers, four miniaturised CMOS camera-based sun sensors, and 6 IMUs positioned strategically to avoid magnetic interference. The attitude control algorithms fuse sensor data and precisely manage the reaction wheels, achieving a 2° pointing accuracy. While further improvements would require star trackers (beyond TOM's scope), our current accuracy suffices for coordinated Earth observation. Orbit control is realized by AOCS by managing a single-axis bi-propellant propulsion system. This system provides over 400 Ns total impulse, covering the planned 2-year formation flight lifetime. It also facilitates lowering the orbit altitude at mission end to limit remaining orbit life. Reaction wheels orient the satellite body along three axes. This precise control enhances agility and stability. Orbit determination is implemented by 4 integrated GNSS modules and antennas to ensure redundancy. Raw sensor data collected from these modules feeds onboard propagator

algorithms for future observation planning. Additionally, individual satellite orbital elements are exchanged by the use of Inter Satellite Link (ISL), to have formation structure knowledge on each satellite. The AOCS interfaces with the payload unit, further improving pointing accuracy through visual servoing. A more detailed view on AOCS Design is presented in [11].

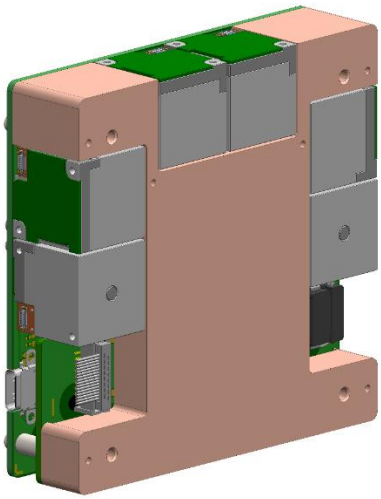

Figure 5 TOM ADCS

3.3 THRUSTER

The propulsion is a pivotal subsystem in identifying formation acquisition and maintenance efforts. TOM satellites must be able to provide similar orbit manoeuvrability to each other, and thus each satellite's propulsion subsystem must provide similar delta-v and have the maximum thrust acceleration in similar range. To distribute formation control efforts fairly between different satellites, each satellite would be able to deliver enough delta-v to acquire and maintain the TOM formation as if the other satellites are passive in coordination. A chemical propulsion unit from Dawn Aerospace was considered due to volume, power requirements, performance, and technology readiness level (TRL). The bi-propellant chemical propulsion unit occupies 0.8U of volume, provides total impulse of 405Ns, and uses Propylene/Propene (C3H6) as fuel with Nitrous oxide (N2O) as oxidizer. [13]

3.4 COMMUNICATION SUBSYSTEM (COM)

Effective communication is the lifeline of any satellite mission. The TOM satellite relies on two primary communication channels: UHF (Ultra High Frequency) and S-band. The UHF channel serves for TMTC between the ground station and the satellite. This same communication unit also plays a crucial role in establishing inter-satellite links. During the NetSat mission, we demonstrated its capability to extend communication distances between satellites of more than 100 km [22, 9], while maintaining robust link quality. Over this link orbital positions, basic data about observation targets, and critical updates are exchanged seamlessly. The S-band channel handles the downlink of scientific payload data. Specifically, the S-band communication unit interfaces with the payload computer, ensuring efficient data transfer. Stored images captured by TOM's multi-channel visible spectrum camera are transmitted via this S-band link. The large lobe width of the patch antenna allows for a coarse alignment (around 10°) while maintaining a strong link quality. To validate this communication link, rigorous field tests were conducted on the ground. Distances of up to 3000 km were simulated by using additional attenuators.

4 FORMATION ANALYSIS

When designing satellite formations for Earth observation missions, several key considerations come into play. These include achieving optimal imaging conditions, such as ensuring consistent cross-track baselines or maintaining relative motion by considering the dynamics and orbit-specific disturbances. The objective of the TOM formation design is to obtain a three-dimensional view of a ground target. Consequently, establishing and consistently maintaining a significant cross-track baseline is crucial for enhancing the resolution of the 3D image data. The force-free path satellites perform while flying in a formation can be separated into in- and out-of-orbital plane motion. For TOM a constant offset between the satellites would be best. In-plane this can be achieved with an along-track separation primarily by changing the argument of latitude with similar eccentricities and no difference in altitude. A continuous Out-of-Plane positioning between two satellites is not possible. However, a pendulum motion can be achieved by adjusting the inclination or the Right Ascension of the Ascending Node (RAAN). Two possible out-of-plane scenarios are considered for the TOM mission. One option is to fly all three satellites with a fixed along-track separation, and one of the satellites gets an additional RAAN difference to create a pendulum motion.
The second scenario also consists of three satellites flying with a fixed along-track separation. Still, all satellites are placed in a pendulum motion towards the reference orbit with different phase shifts between them.
The selected reference orbit is a Sun-Synchronous Orbit (SSO) on an altitude of 525 km and an inclination of 97.5 degrees. Each satellite's relative orbit is defined as Relative Orbital Elements (ROE) because it represents the created relative orbit rather explicitly. An ROE $\delta\alpha = (\delta a, \delta\lambda, \delta e_x, \delta e_y, \delta i_x, \delta i_y)^T$ consists out of the altitude difference δa, the along-track separation $\delta\lambda$ the relative eccentricity $\delta e = (\delta e_x, \delta e_y)$ and the relative inclination $\delta i = (\delta i_x, \delta i_y)$. The relative eccentricity and inclination consist of two values, which define the amplitude and phase of each pendulum behaviour for the in-plane and out-of-plane motion. [5, 14]
For the RAAN-only scenario, the relative reference orbits are

$$a\delta\alpha_1 = \begin{pmatrix} 0 \\ 75km \\ 0 \\ 0 \\ 0 \\ -35km \end{pmatrix}, \qquad a\delta\alpha_2 = \begin{pmatrix} 0 \\ 0 \\ 0 \\ 0 \\ 0 \\ 35km \end{pmatrix}, \qquad a\delta\alpha_3 = \begin{pmatrix} 0 \\ -75km \\ 0 \\ 0 \\ 0 \\ -35km \end{pmatrix}.$$

This results in a RAAN difference of 0.29° for each satellite to the reference orbit. The second scenario, with all three satellites oscillating with different phases, is

$$a\delta\alpha_1 = \begin{pmatrix} 0 \\ 75km \\ 0 \\ 0 \\ 35km \\ 0 \end{pmatrix}, \qquad a\delta\alpha_2 = \begin{pmatrix} 0 \\ 0 \\ 0 \\ 0 \\ 17.5km \\ -30.3km \end{pmatrix}, \qquad a\delta\alpha_3 = \begin{pmatrix} 0 \\ -75km \\ 0 \\ 0 \\ 17.5km \\ 30.3km \end{pmatrix}.$$

This results for the first satellite in an inclination difference of 0.29°, and for the second and third, an inclination difference of 0.14° and for the RAAN difference of 0.25°.
The ROE states are transformed into initial Local Vertical Local Horizontal (LVLH) states to evaluate both scenarios on the Clohessy-Wiltshire Equations ([4] equation 7.42) to observe the relative motion in the Radial, Tangential, and Normal direction of the reference orbital plane. Since the formation has a relatively large baseline, which exceeds the limitations of the linearization, further correction terms

regarding the curvature of the orbit have to be included for a more detailed analysis of perturbations. However, it is sufficient for an approximation of the observational capabilities of each formation. Figure 6 displays the relative position towards the reference orbit and the baselines between every satellite pair. If you compare scenario 1, displayed in Figures 6a and 6c, with scenario 2, which are displayed in Figures 6b and 6d, the difference is in the phase shift of the Out-of-Plane or Cross-Track motion. For the RAAN-only scenario 1, there is no phase difference between satellites 1 and 3 and a phase difference of 180° towards satellite 2. Therefore, twice in each orbit, there is no third-dimension displacement in the observation, and a photogrammetric reconstruction is impossible. For scenario 2, the phase shift between each satellite is evenly distributed and corresponds
to 120 degrees. This leads to a more robust cross-track baseline. By comparing the cross-track baseline of scenarios 1 and 2, it is apparent that the baseline is about 10 km bigger at a maximum for the RAAN-only scenario. However, for the 3-pendulum-formation, the cross-track baseline never drops below 52.5 km over the entire orbit; thus, the cross-track baseline is over 55 percent of the orbit larger than in scenario 1. Analysing the overall distances between the satellite pairs in all 3 dimensions, the baselines look fairly similar for both scenarios: over 150 km for the far satellite pair and around 90 km for the close pairs.

Addressing the baselines mentioned above in Figure 4, the total height resolution for the three-dimensional baseline is around 100 meters at the 20 meters GSD of the payload. However, for the cross-track baseline, the height resolution varies a lot between both scenarios due to the reciprocal nature of the resolution. Scenario 2, therefore, offers a stable resolution over the entire orbit, while scenario 1 fails to do so. This is why solely focusing on RAAN adjustments may not be ideal for continuous imaging, while the 3-pendulum configuration provides good coverage for most of the Earth while flying in an SSO. For example, the location and timing of an ash cloud resulting from a volcanic eruption cannot be predicted and can occur in unfavourable places on the Earth. Therefore, the formation cannot record this event to a sufficient quality.

In contrast to the benefits this idealised formation in scenario 2 offers, there are also some draw backs that have to be discussed and two important ones relate to the change in inclination. As an estimate for the additional cost for the establishment of the formation the equations for the jump conditions in [8] are utilized. Rearranged, for the Δv requirement of the determined change in RAAN and inclination, the equations look like

$$\Delta v_z = \frac{\Delta i}{\gamma \cos \theta_i} + \frac{\Delta \Omega \sin i_0}{\gamma \sin \theta_\Omega}$$

, where $\gamma = \sqrt{\frac{a}{\mu}}$, and θ_i, θ_Ω as the argument of latitude of the required impulse can be placed optimally during an orbit. For scenario 1 the Δv for each satellite is 38.34 m s and for scenario 2 the required Δv for the first satellite is also 38.34 m s and for the second and third are 51.56 m s. Hence the second scenario requires roughly 23% more fuel. Another draw-back for the second scenario is that the inclination is precisely chosen for the necessary RAAN drift on this altitude to maintain the SSO. Additionally, the relative RAAN-drift between the satellites have to be managed to maintain the formation which also raises additional thrust cost. In conclusion, it can be said that the alternative scenario provides significant advantages in the observation of the Earth, but it must be reviewed whether it fits into the budget of the mission.

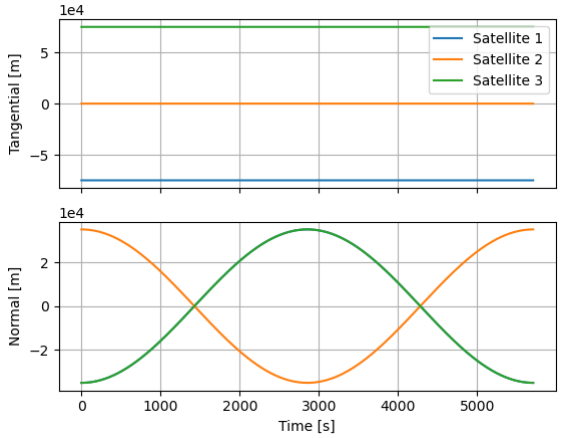

(a) Relative Motion in the Tangential and Normal Direction of Three Satellites Flying in a RAAN-Only-Pendulum Formation

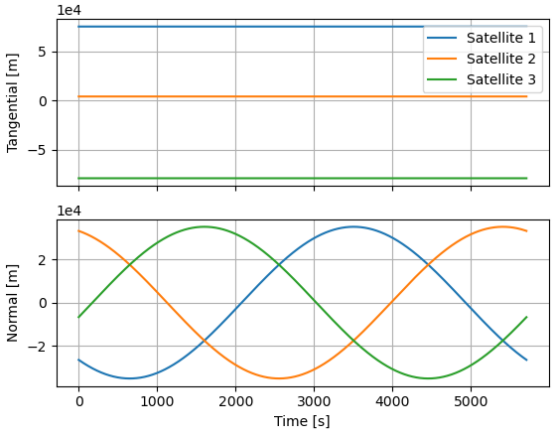

(b) Relative Motion in the Tangential and Normal Direction of Three Satellites Flying in an equally Spaced 3-Pendulum-Formation

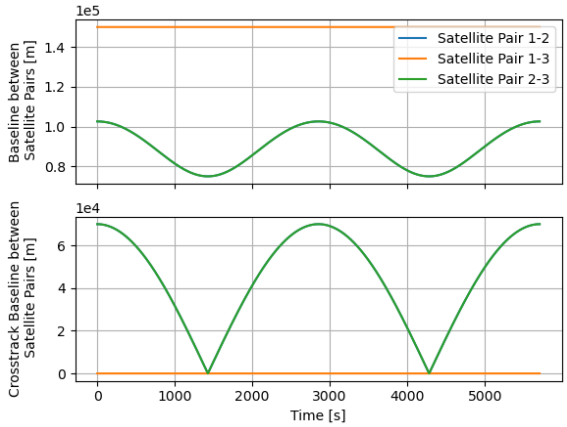

(c) The Global and Cross-Track Baseline between each Satellite Pair Flying in a RAAN-Only-Pendulum Formation

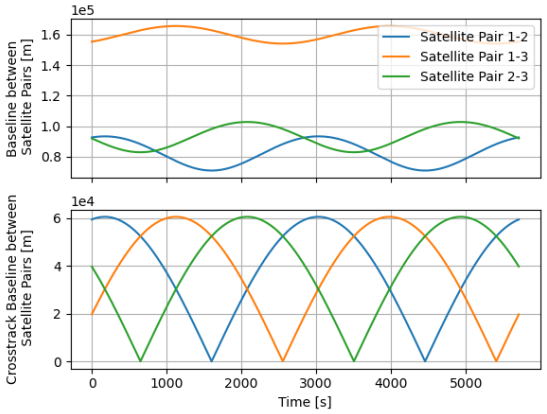

(d) The Global and Cross-Track Baseline between each Satellite Pair Flying in a 3-Pendulum-Formation

Figure 6 Relative Motion and Resulting Baselines of the possible TOM-Formations evaluated on the initial States in LVLH with the Clohessy-Wiltshire Equations

5 VISION-BASED ATTITUDE CONTROL

Taking advantage of the camera payload a technology evaluation experiment addresses a vision-based attitude control approach to be demonstrated in TOM. A similar approach, based on detection and matching of landmarks in camera images, was successfully applied by the Mars 2020 Entry, Descent and Landing system to deliver the Perseverance rover to the Mars surface. In comparison to the previously used conventional navigation methods, the vision-based system was able to improve the position estimation accuracy from about 3 km to the order of a few meters, unlocking new landing sites on Mars which would otherwise be unattainable because of their hazardous environments including cliffs, dune fields and rocks[12]. Another new aerospace application of such vision-based methods is the development of GPS-denied drones which calculate their position by matching their camera images to satellite imagery [19]. Vision-based control in general originates from the field of robotics where it is called visual servoing.

5.1 BASIC PRINCIPLE OF RELATIVE VISUAL SERVOING

The vision-based control approach developed for TOM aims at maximizing the jointly observed target area of all satellites in the formation. This goal is achieved by controlling the satellites' attitudes relative to each other in order to have all of them point at the same Earth surface target. Hence, this control method is referred to as relative visual servoing. The basic principle of relative visual servoing is illustrated in Figure 7. One of the satellites is assigned the role of the leader which defines the ground target to be jointly observed. The other two satellites - designated as follower satellites - then have to point to the target defined by the leader.

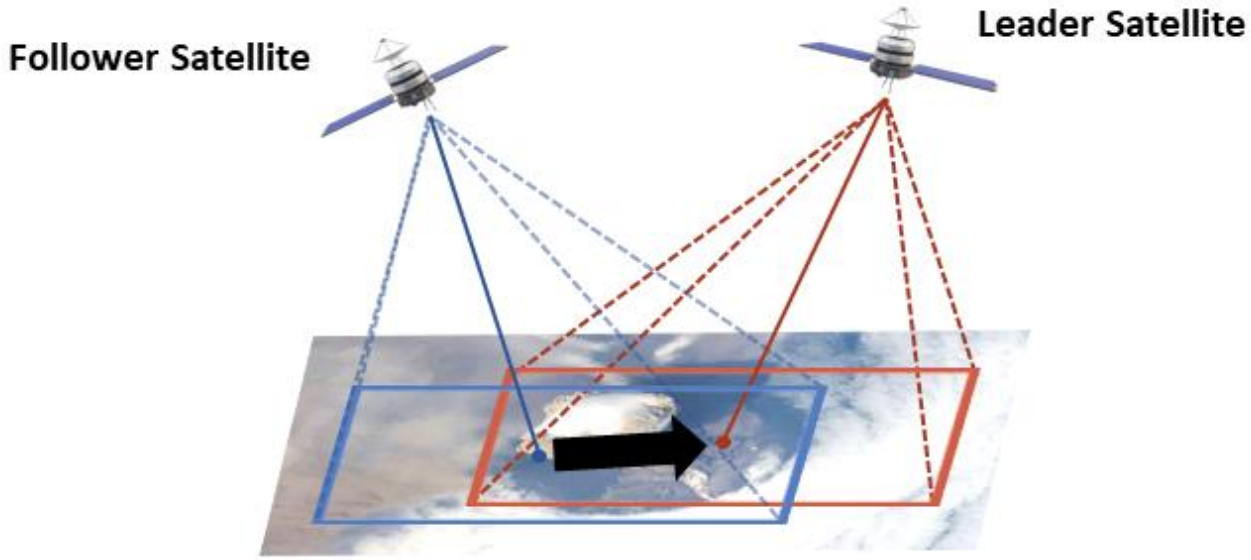

Figure 7: Basic Principle of Relative Visual Servoing

5.2 MAIN PROCESSING STEPS

A detailed derivation and description of the relative visual servoing approach can be found in [6] and [10]. Thus, the functionality is only briefly presented in the following. Figure 8 shows the main processing steps of relative visual servoing for TOM. At the beginning of an overflight over the observation target, each satellite performs a coarse pointing toward the target using the conventional Attitude Determination and Control System (ADCS) sensors. As soon as the course pointing is established, the leader satellite starts the visual servoing procedure. First of all, in the feature initialization step, the leader identifies so-called features in the first two camera images. Features are unique points in an image that are different from their immediate neighbourhood and can, therefore, be detected in subsequent images of the scenery. Further characteristics of features are the invariance to geometric changes (e.g., translation, scaling, or rotation) as well as to photometric changes (e.g., in brightness or exposure), enabling their reliable detection from different viewing directions and distances. The detected features are used as reference features in the following steps. Therefore, they are also sent to the follower satellites via the ISL. [20]

The following steps are executed onboard all satellites in the formation. After the feature initialization is completed, the reference features are tracked in the newly captured images. The image positions of the reference features and the matched features from the current image are used to calculate the error angles. This is done by calculating the differences between the initial positions of the reference features in the first image and their tracked positions in the current image. The resulting pixel shifts can be converted to error angles around roll, pitch, and yaw. While the steps described before are conducted on the payload computer, the error angles are sent to the AOCS for the last step. There,

the controller (e.g., quaternion-based Linear–Quadratic Regulator (LQR)) calculates the corresponding control torque, which is then applied by the reaction wheels

5.3 TESTING

For verification and further improvement of the visual servoing approach, different test environments are used. For fast testing without the need to set up a complex test environment involving hardware, a solely software-based setup is available. To visualize the satellite's camera, an Earth Observation Simulator generates simulated images based on a given orbit position and camera pointing direction, which are then fed into the visual servoing algorithm.

Figure 9 shows two more complex HiL test setups involving the actual hardware. For the test setup on the left, the Earth Observation Simulator is used to generate satellite imagery, which is projected on a wall by a beamer. The advantage of this setup is the inclusion of the actual cameras in the test, ensuring a more realistic test scenario. On the right, the turntable test setup is depicted. The CubeSats or corresponding models, including cameras, are mounted on the two high-precision turntables, simulating the angular movement of the satellites. Between these two turntables, a mobile robot moves the observation target, a 3D-printed volcano model, which is used to test the cooperative target tracking. A wi-fi or cable connection simulates the ISL between the two satellites.

The simulations and tests in the different testing environments demonstrate the feasibility of the relative visual servoing approach. For the cooperative tracking, a relative pointing accuracy well below 0.1° was achieved [6]. These results correspond well to the theoretical analysis of all error contributors and corresponding error mapping for the visual servoing approach, indicating a feasible pointing accuracy of about 0.05° [15]. Nevertheless, since some effects - like atmospheric disturbances and cloud coverage - cannot be realistically simulated on-ground, in-orbit testing is essential to prove the readiness of the technology for space applications.

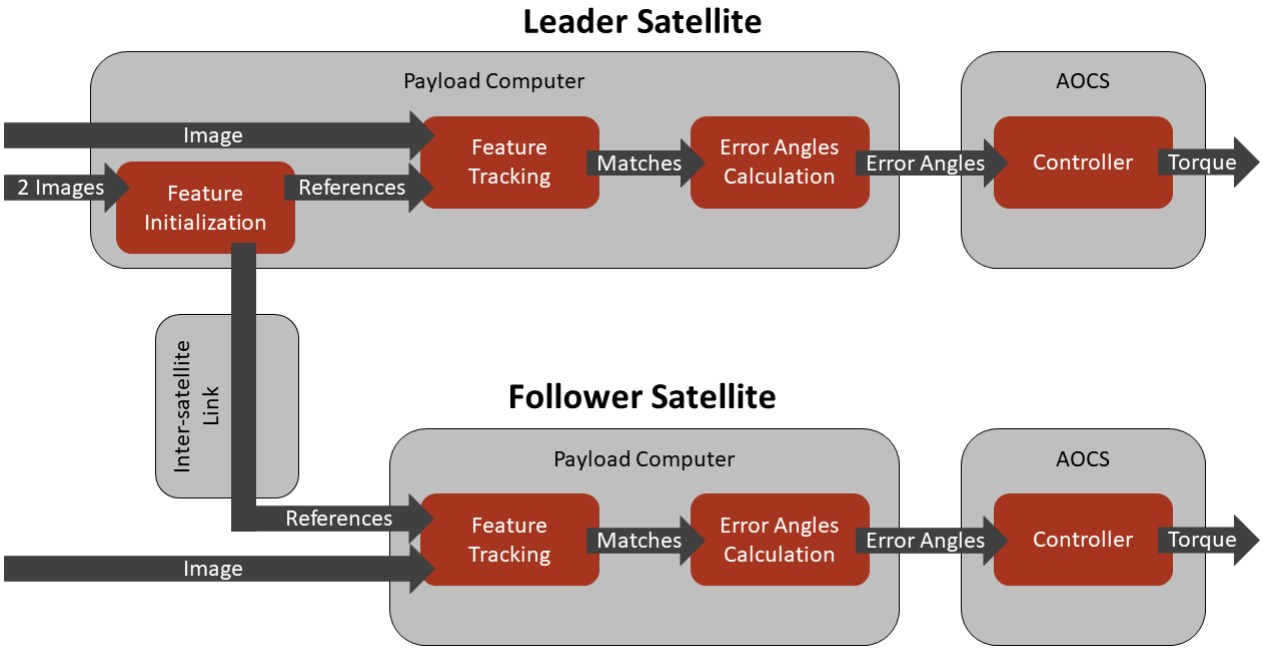

Figure 8 Main Processing Steps of Relative Visual Servoing for TOM

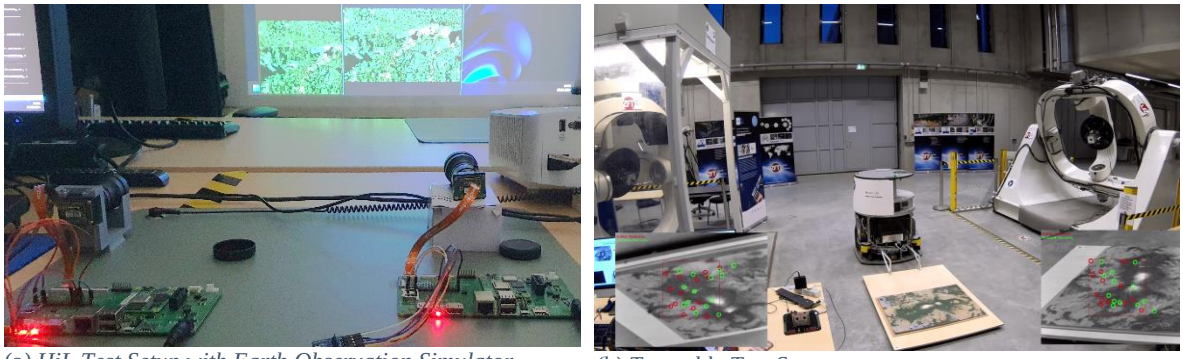

(a) *HiL Test Setup with Earth Observation Simulator* *(b) Turntable Test Setup*

Figure 6 HiL Test Setup for Visual Servoing

5.4 ABSOLUT VISUAL SERVOING

In addition to the relative visual servoing control approach for cooperative tracking, another vision-based method for the determination of the (”absolute”) attitude and position of the satellite in the Earth-Centered Inertial (ECI) frame will be tested in TOM. [7] This way, the satellite’s camera serves as a sort of additional sensor for attitude and position determination. In the following, this approach is referred to as absolute visual servoing. Figure 10 illustrates the basic principle of absolute visual servoing: Features detected in the satellite’s images are matched with known Ground Control Points (GCPs) stored in an on-board database, which has been generated and optimized before on-ground. Therefore, a reference between pixel positions in the camera images and geographic positions on the Earth’s surface (given in the Earth-Centered Earth-Fixed (ECEF) frame) is found. This information is then used to calculate the position and attitude of the camera with respect to the ECI frame using the collinearity equations and transforming to the desired
reference frame.

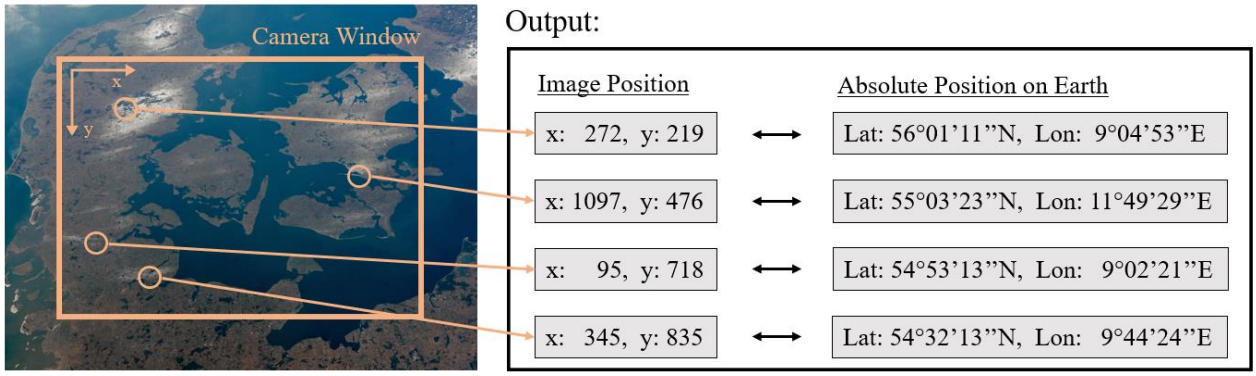

Figure 10 Basic Principle of Absolute Visual Servoing

6 CONCLUSION

The TOM satellite mission will analyse the 3D-features on the Earth surface by a formation of 3 nano-satellites. The satellite system design addresses the challenges including the realisation of self-organizing satellite formation through networked control, as well as joint precision pointing suitable for subsequent photogrammetric processing within the limited resources of nano-satellite. Additionally, the vision-based attitude control experiment for TOM has been further outlined, promising more precise coordinated pointing for the tracking of ground targets. Extensive simulations and HiL-tests were performed on attitude control. Simultaneously, efforts continue to expand the

ground station network and optimize scientific data processing with the support of the RLS international partner network. The hardware integration of three satellites is completed, and performance test provide confidence for appropriate performance in orbit. The 3 satellites are now stored in the cleanroom and wait for their launch opportunity at end of 2024.
Thus, TOM will soon provide data to geo-scientists for research to improve understanding of our planet.

7 ACKNOWLEDGEMENTS

The authors thank all international collaborators of the RLS Science Project Small Satellites for their contributions. The authors gratefully acknowledge the support of TOM by the Bavarian Ministry of Economic Affairs. We thank the DLR e.V. for the generous funding of the SciTOM as well as the Bayerisches Staatsministerium für Wirtschaft, Landesentwicklung und Energie for its ongoing support in the OperaTOM project.

8 REFERENCES

[1] Alfriend, K. T. ; Vadali, S. R. ; Gurfil, P. ; How, J. P. ; Breger, L. : Spacecraft formation flying: Dynamics, control and navigation. Bd. 2. Elsevier, 2009

[2] Busch, S. ; Schilling, K. : Standardization Approaches for Efficient Electrical Interfaces of CubeSats. In: integration 3 (2016), Nr. 4, S. 5

[3] Carvalho, R. A. ; Estela, J. ; Langer, M. : Nanosatellites: Space and Ground Technologies, Operations and Economics. John Wiley & Sons, 2020

[4] Curtis, H. D.: Orbital mechanics for engineering students. 1. ed., reprinted. Amsterdam Heidelberg : Elsevier Butterworth Heinemann, 2008 (Elsevier Aerospace engineering series). – ISBN 978–0–7506–6169–0

[5] D'Amico, S. ; Montenbruck, O. : Proximity Operations of Formation-Flying Spacecraft Using an Eccentricity/Inclination Vector Separation. In: Journal of Guidance, Control, and Dynamics 29 (2006), Mai, Nr. 3, 554–563. http://dx.doi.org/10.2514/1.15114. – DOI 10.2514/1.15114. – ISSN 0731–5090, 1533–3884

[6] Dauner, J. ; Elsner, L. ; Ruf, O. ; Borrmann, D. ; Scharnagl, J. ; Schilling, K. : Visual servoing for coordinated precise attitude control in the TOM small satellite formation. In: Acta Astronautica 202 (2023), 760-771. http://dx.doi.org/https://doi.org/10.1016/j.actaastro. 2022.10.003. – DOI https://doi.org/10.1016/j.actaastro.2022.10.003. – ISSN 0094–5765

[7] Dauner, J. ; Redelbach, J. ; Elsner, L. ; Mammadov, I. ; Schilling, K. : Absolute Visual Servoing for Precise Earth Target Pointing Onboard Small Satellites. In: Proceedings of the 74th International Astronautical Congress (IAC). Baku, Azerbaijan, 2023

[8] D'Errico, M. (Hrsg.): Distributed Space Missions for Earth System Monitoring. Springer New York. http://dx.doi.org/10.1007/978-1-4614-4541-8. http://dx.doi.org/10.1007/978-1-4614-4541-8. – ISBN 978–1–4614–4540–1 978–1–4614–4541–8

[9] Dombrovski, S. ; Scharnagl, J. ; Schilling, K. : Experience with Compass-based IoT approach used in NetSat formation mission. (2021)

[10] Elsner, L. : Development and Integration of Cooperative Vision-Based Attitude Control for the TOM Mission, University of Würzburg, Masterthesis, 2022

[11] Elsner, L. ; Petermann, T. ; Arnim, M. von ; Schilling, K. : Pre-flight verification of the CubeSat Attitude Control System for the QUBE mission. In: Small Satellites Systems and Services (4S) Symposium, 2024

[12] Johnson, A. E. ; Cheng, Y. ; Trawny, N. ; Montgomery, J. F. ; Schroeder, S. ; Chang, J.; Clouse, D. ; Aaron, S. ; Mohan, S. : Implementation of a Map Relative Localization System for Planetary Landing. In: Journal of Guidance, Control, and Dynamics 46 (2023), Nr. 4, 618-637. http://dx.doi.org/10.2514/1.G006780. – DOI 10.2514/1.G006780

[13] Kleinschrodt, A. ; Motroniuk, I. ; Aumann, A. ; Mammadov, I. u. a.: TIM: An International Formation for Earth Observation with CubeSats. In: 12th IAA Symposium on Small Satellites for Earth Observation, 2019

[14] Koenig, A. W. ; Guffanti, T. ; D'Amico, S. : New State Transition Matrices for Relative Motion of Spacecraft Formations in Perturbed Orbits. In: AIAA/AAS Astrodynamics Specialist Conference. American Institute of Aeronautics and Astronautics. – ISBN 978–1–62410–445–9

[15] Kumar, P. : Statistical Analysis of Error Contributors and Error Mapping for Enhanced Pointing Accuracy of Multi-satellite Missions, University of Würzburg, Diplomarbeit, 2024

[16] Mathavaraj, S. ; Padhi, R. : Satellite Formation Flying: High Precision Guidance Using Optimal and Adaptive Control Techniques. Springer Nature, 2021

[17] Millan, R. ; M. Ariel, R. S. ; Bartalev, S. ; Borgeaud, M. ; Campagnola, S. ; Castillo-Rogez, J. ; Fleron, R. ; Gass, V. ; Gregorio, A. ; Lal, D. K. B. ; MacDonald, M. ; Park, J. H. ; Rao, V. S. ; Schilling, K. ; Stephens, G. ; Title, A. ; Wu, J. : Small satellites for space science: A COSPAR scientific roadmap. In: Advances in space research 64 (2019), Nr. 8, S.1466–1517

[19] Reim, G. : How A Trio Of Engineers Developed A GPS-Denied Drone For Under $500. In: Aviation Week (2024). https://aviationweek.com/aerospace/emerging-technologies/how-trio-engineers-developed-gps-denied-drone-under-500

[20] Ruf, O. ; von Arnim, M. ; Kempf, F. ; Haber, R. ; Elsner, L. ; Dauner, J. ; Dombrovski, S. ; Kramer, A. ; Schilling, K. : Advanced test environment for automated attitude control testing of fully integrated CubeSats on system level. In: CEAS Space Journal (2023), Okt. http://dx.doi.org/10.1007/s12567-023-00523-x. – DOI 10.1007/s12567–023–00523–x

[21] Sandau, R. : Novel ideas for nanosatellite constellation missions. International Academy of Astronautics, 2012

[22] Scharnagl, J. ; Haber, R. ; Dombrovski, V. ; Schilling, K. : NetSat—Challenges and lessons learned of a formation of 4 nano-satellites. In: Acta Astronautica 201 (2022), S. 580–591

[23] Schilling, K. : Perspectives for miniaturized, distributed, networked cooperating systems for space exploration. In: Robotics and Autonomous Systems 90 (2017), S. 118–124

[24] Schilling, K. ; Loureiro, G. ; Zhang, Y. ; Nüchter, A. ; Scharnagl, J. ; Motroniuk, I. ; Aumann, A. : TIM: An International Nano-Satellite Formation for Photogrammetric Earth Observation. (2019)

[25] Zaksek, K. ; James, M. R. ; Hort, M. ; Nogueira, T. ; Schilling, K. : Using picosatellites for 4-D imaging of volcanic clouds: Proof of concept using ISS photography of the 2009 Sarychev Peak eruption. In: Remote Sensing of Environment 210 (2018), S. 519–530

[26] Zurbuchen, T. ; Steiger, R. von ; Bartalev, S. ; Dong, X. ; Falanga, M. ; Fleron, R. ; Gregorio, A. ; Horbury, T. S. ; Klumpar, D. ; Küppers, M. ; Macdonald, M. ; Millan, R. ; Petrukovich, A. ; Schilling, K. ; Wu, J. ; Yan, J. : Performing high-quality science on cubesats. In: Space Research Today 196 (2016), S. 11–30